Targeting EF-hand domain family member D1 (EFHD1) in liver disease

David Eberhardt[1], Ashley Bratt[1], David Mollinedo[1], Sandra Lee[1], Sihem Boudina[2], Kimberley Evason[3], Dipayan Chaudhuri[1,4]

[1]Nora Eccles Harrison Cardiovascular Research and Training Institute (CVRTI), University of Utah; [2]Nutrition & Integrative Physiology, University of Utah; [3]Anatomic Pathology, University of Utah; [4]Department of Biochemistry, Department of Biomedical Engineering, University of Utah

BACKGROUND: New treatments for liver disease may arise by examining genes identified in genome-wide association studies (GWAS). Variation in one such gene, EF-hand domain family member D1 (EFHD1), has been associated with liver injury biomarkers in multiple GWAS analyses[1-8]. In these studies, higher serum biomarkers correlate with increased EFHD1 expression. EFHD1 is a poorly studied mitochondrial Ca^{2+}-binding protein, and how it regulates liver function is unknown. We sought to assess whether inhibiting hepatic EFHD1 could represent a novel therapy for treating metabolic liver disease.

METHODS:

1. *Efhd1*-knockout (*Efhd1*$^{-/-}$) mice were obtained from the Jackson Laboratory.
2. Hepatocytes were isolated via the 2-step isolation method[9].
3. Mice were fed a High fat diet (HFD) or Gubra-Amylin NASH (GAN) diet for 28 weeks.

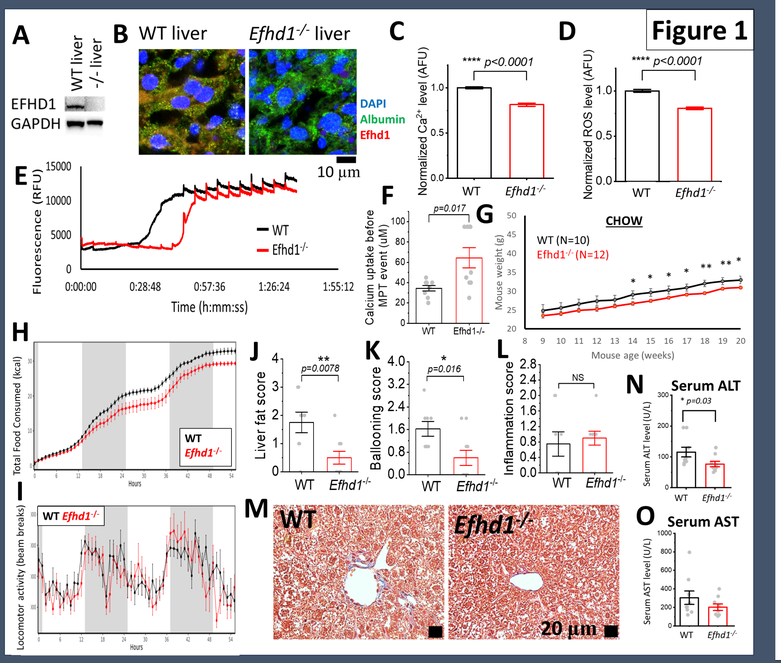

Figure 1: EFHD1 in the liver.

A. Western blot showing that EFHD1 is absent in *Efhd1*$^{-/-}$ mouse liver.

B. Immunohistochemistry showing that EFHD1 is present in hepatocytes. Samples are slices from WT and *Efhd1*$^{-/-}$ mouse livers. Staining is for DAPI (blue), Albumin (hepatocyte marker, green), EFHD1 (red).

C, D. Mitochondrial calcium levels (C) and mitochondrial ROS levels (D) in isolated hepatocytes from WT and *Efhd1*$^{-/-}$ mouse livers.

E, F. Calcium retention capacity of liver mitochondria from WT and *Efhd1*$^{-/-}$ mice.

G. Weight gain over time of male WT and *Efhd1*$^{-/-}$ mice.

H, I. Recordings of food intake (H) and locomotor activity (I) from WT and *Efhd1*$^{-/-}$ mice over 54 hours in a metabolic cage.

J. Comparison of liver fat scoring from histology slides of WT and *Efhd1*$^{-/-}$ mouse liver.

K. Comparison of hepatocyte ballooning scoring from histology slides of WT and *Efhd1*$^{-/-}$ mouse liver.

J. Comparison of inflammation scoring from histology slides of WT and *Efhd1*$^{-/-}$ mouse liver.

M. Exemplar histology images of WT and *Efhd1*$^{-/-}$ mouse liver. Trichrome stain.

N, O. ALT and AST levels in serum from WT and *Efhd1*$^{-/-}$ mice.

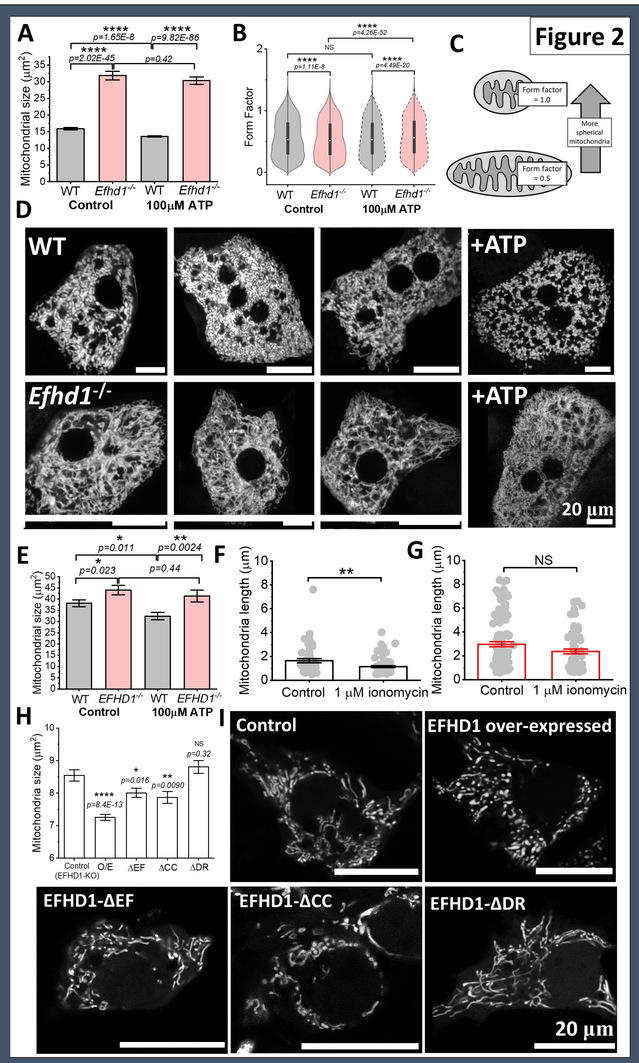

Figure 2: EFHD1 ablation alters mitochondrial morphology in liver cells and prevents calcium-induced changes in mitochondrial morphology.

A. Comparison of mitochondrial size in hepatocytes isolated from WT and *Efhd1*$^{-/-}$ mice in the presence and absence of ATP.

B. Comparison of mitochondrial form factor in hepatocytes isolated from WT and *Efhd1*$^{-/-}$ mice in the presence and absence of ATP.

C. Schematic visually explaining form factor.

D. Exemplar images of isolated hepatocytes from WT and *Efhd1*$^{-/-}$ mice. Cells were isolated <24 hours prior to imaging and cells were treated with Mito tracker orange. 100 μM ATP was added to induce intracellular calcium release.

E. Comparison of mitochondrial size in WT and *EFHD1*$^{-/-}$ HEPG2 cells in the presence and absence of ATP.

F, G. Comparison of mitochondrial length in WT (F) and *EFHD1*$^{-/-}$ (G) HEPG2 cells in the presence and absence of 1 μM ionomycin.

H. Comparison of mitochondrial size in HEPG2 cells lacking EFHD1 (EFHD1-KO), overexpressing EFHD1 (O/E), expressing EFHD1 lacking the EF-hand regions (ΔEF), expressing EFHD1 lacking the coiled-coil region (ΔCC), expressing EFHD1 lacking the intrinsic disordered region (ΔDR).

I. Exemplar images of HEPG2 cells lacking EFHD1 (Control), overexpressing EFHD1 (EFHD1 over-expressed), expressing EFHD1 lacking the EF-hand regions (EFHD1-ΔEF), expressing EFHD1 lacking the coiled-coil region (EFHD1-ΔCC), expressing EFHD1 lacking the intrinsic disordered region (EFHD1-ΔDR). Cells were treated with Mito tracker orange

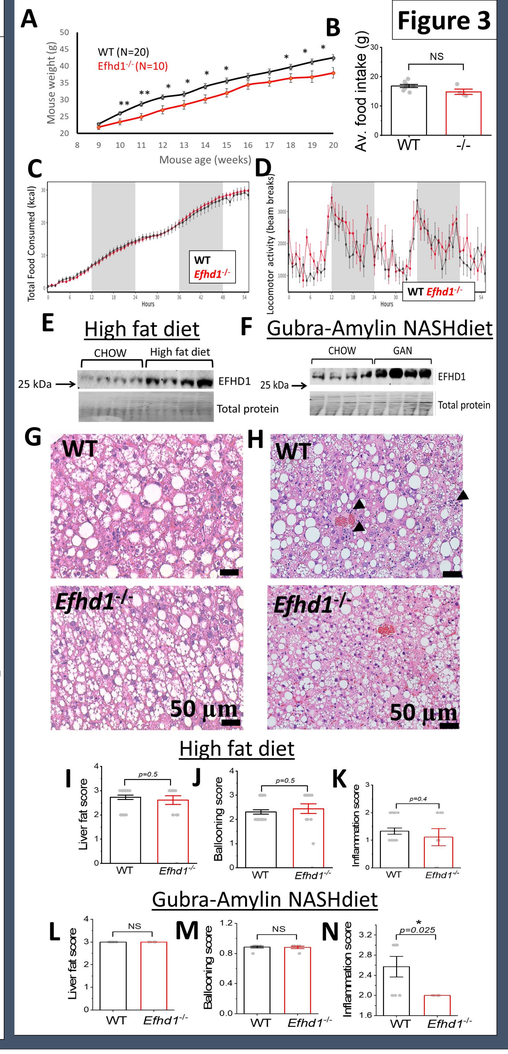

Figure 3: EFHD1 ablation alters weight gain in mice fed a high-fat diet (HFD) and lowers inflammation in mouse livers following a (Gubra-Amylin NASH) GAN diet.

A. Comparison of body weights of male WT and *Efhd1*$^{-/-}$ mice on a HFD over time

B. Comparison of food intake for male WT and *Efhd1*$^{-/-}$ mice on a HFD.

C, D. Recordings of food intake (B) and locomotor activity (C) from WT and *Efhd1*$^{-/-}$ mice over 54 hours in a metabolic cage fed a HFD

E, F. Western blot showing that EFHD1 levels are increased in mouse livers following a HFD (E) or a GAN diet (F).

G, H. Exemplar histology images of WT and *Efhd1*$^{-/-}$ mouse livers following a HFD (G) or a GAN diet (H). Arrows indicate foci caused due to inflammation.

I. Comparison of liver fat scoring from histology slides of WT and *Efhd1*$^{-/-}$ mouse liver following a HFD.

J. Comparison of hepatocyte ballooning scoring from histology slides of WT and *Efhd1*$^{-/-}$ mouse liver following a HFD.

K. Comparison of liver inflammation scoring from histology slides of WT and *Efhd1*$^{-/-}$ mouse liver following a HFD.

L. Comparison of liver fat scoring from histology slides of WT and *Efhd1*$^{-/-}$ mouse liver following a GAN diet.

M. Comparison of hepatocyte ballooning scoring from histology slides of WT and *Efhd1*$^{-/-}$ mouse liver following a GAN diet.

N. Comparison of liver inflammation scoring from histology slides of WT and *Efhd1*$^{-/-}$ mouse liver following a GAN diet.

CONCLUSIONS:

1. EFHD1 ablation was beneficial in liver mitochondria (Figure 1C-1F) and led to healthier mouse livers at baseline (Figure 1G-1O).
2. EFHD1 ablation resulted in larger mitochondria in isolated mouse hepatocytes and HEPG2 cells and inhibited the morphological effect of calcium. The EF-hand and coiled-coil regions of the protein were required for these morphological effects (Figure 2).
3. *Efhd1*$^{-/-}$ mice on a HFD gained weight slower than their WT counterparts which was independent of food intake or activity (Figure 2A-3C). Conversely, slower weight gain corresponding to lower food intake was observed in mice fed a CHOW diet (Figure 1G, 2H)
4. EFHD1 expression was increased in mouse livers following a HFD or GAN diet (Figures 3E, 3F), and EFHD1 ablation lowered inflammation in mouse livers following a GAN diet, but not a HFD (Figure 3G-3N)

Funding: DMRC Larry H Miller Driving Out Diabetes and Nora Treadwell Eccles Foundation for financial support seed grant and American Heart Association Postdoctoral Fellowship grant

References: [1] Hakim *et al.*, Genetic Variation in the Mitochondrial Glycerol-3-Phosphate Acyltransferase Is Associated With Liver Injury. Hepatology, 2021. 74(6): p. 3394-3408. **[2]** Pazoki *et al.*, Genetic analysis in European ancestry individuals identifies 517 loci associated with liver enzymes. Nat Commun, 2021. 12(1): p. 2579. **[3]** Ward *et al.*, GWAS of serum ALT and AST reveals an association of SLC30A10 Thr95Ile with hypermanganesemia symptoms. Nat Commun, 2021. 12(1): p. 4571. **[4]** Chambers *et al.*, Genome-wide association study identifies loci influencing concentrations of liver enzymes in plasma. Nat Genet, 2011. 43(11): p. 1131-8. **[5]** Kanai *et al.*, Genetic analysis of quantitative traits in the Japanese population links cell types to complex human diseases. Nat Genet, 2018. 50(3): p. 390-400. **[6]** Sakaue *et al.*, A cross-population atlas of genetic associations for 220 human phenotypes. Nat Genet, 2021. 53(10): p. 1415-1424. **[7]** Chen *et al.*, Genome-wide association study of serum liver enzymes implicates diverse metabolic and liver pathology. Nat Commun, 2021. 12(1): p. 816. **[8]** Currin *et al.*, Genetic effects on liver chromatin accessibility identify disease regulatory variants. Am J Hum Genet, 2021. 108(7): p. 1169-1189. **[9]** Suryaprakash *et al.*, CerS2 Haploinsufficiency Inhibits β-Oxidation and Confers Susceptibility to Diet-Induced Steatohepatitis and Insulin Resistance. Cell Metabolism, 2014. 20(4):p. 687-695